Molecular Orientation and Conformation of Phosphatidylinositides in Membrane Mimetics Using Variable Angle Sample Spinning (VASS) NMR

Anita I. Kishore and James H. Prestegard
Complex Carbohydrate Research Center, University of Georgia, Athens, Georgia 30602

ABSTRACT For many biological molecules, determining their geometry as they exist in a membrane environment is a crucial step in understanding their function. Variable angle sample spinning (VASS) NMR provides a new route to obtaining geometry information on membrane-associating molecules; it has been used here to scale and separate anisotropic contributions to phosphorus chemical shifts in NMR spectra of phosphatidylinositol phosphates. The procedure allows spectral assignment via correlation with isotropic chemical shifts and determination of a family of probable headgroup orientations via interpretation of anisotropic shift contributions. The molecules studied include phosphtidylinositol-4-phosphate (PI(4)P) and phosphatidylinositol 4,5-bisphosphate (PI(4,5)P_2). A membrane-like environment is provided by a dispersion of alkyl-poly(ethylene) glycols and *n*-alcohols that forms a field-orienting liquid crystal with a director that can be manipulated by varying the sample spinning axis. The experiments presented indicate that the variable angle sample spinning method will provide a direct approach for assignment and extraction of structural information from membrane-associating biomolecules labeled with a wider variety of NMR active isotopes.

INTRODUCTION

NMR methods of structure determination offer much promise for the study of biomolecules embedded in membrane environments. Among other factors, they do not require the molecules of interest to crystallize, and media resembling native membrane systems can be used. Despite recent advances in both high-resolution solution and solid-state NMR spectroscopy, however, characterizing strongly ordered biomolecules remains a challenging task. Here we present an NMR-based method for the study of membrane-associating systems that allows the integration of high-resolution solution NMR chemical shift assignments with the angular information accessible in oriented systems. The applications presented here are on simple phosphatidylinositol phosphates embedded in membrane arrays, but extension to membrane protein systems is possible.

Previous NMR-based investigations have produced a limited number of structures for membrane-associating proteins. Multidimensional solution NMR methods have been applied to characterize membrane proteins in detergent micelles (Almeida and Opella, 1997; Arora et al., 2001; Fernandez et al., 2001; Patzelt et al., 1997). These methods take advantage of multiple pulse, triple resonance experiments developed for soluble proteins to extract high-resolution structural information from uniformly labeled systems. The high radius of curvature of the micelle, however, can raise concerns that its shape may not reflect the native structure (Chou et al., 2002) or the true state of oligomerization of a membrane-bound protein (Vinogradova et al., 1997). Additionally, all orientational information is lost due to the isotropic tumbling of the solubilized protein. High-resolution, triple resonance solid-state experiments have also been developed recently for microcrystalline, powder samples (Pauli et al., 2001; Rienstra et al., 2000, 2002). They offer robust resonance assignment techniques and structural information akin to high-resolution solution methods, but technical challenges remain due to the need for very fast spinning rates and high radio frequency power levels. As with solution NMR experiments, information on orientation is lost. Solid-state NMR methods applicable to oriented assemblies also exist. When these techniques are applied to samples aligned in extended bilayers, both orientational and structural features emerge. Pattern matching techniques have been added to earlier work that depended on the introduction of small numbers of labeled sites (Marassi and Opella, 1998). These new techniques have allowed work with some uniformly labeled helical peptides and membrane protein fragments (Marassi and Opella, 2000; Wang et al., 2000); however, samples must be oriented on glass plates, limiting the sample size and sensitivity. Solid-state NMR studies of lipids in ordered membranes are more numerous (Seelig, 1978), but the technical limitations remain for lipid applications as well.

The approach presented here extracts conformation-dependent offsets from the chemical shift using variable angle sample spinning (VASS). Unlike magic angle spinning in solid-state NMR, in which the sample is fixed at one angle with respect to the magnetic field, in VASS, the rotation axis varies. VASS can be used both to scale and to separate anisotropic contributions to spectra in compounds ordered in liquid crystalline arrays (Courtieu et al., 1994). The isotropic contributions can be correlated with solution or high-resolution solids spectra to make resonance assignments, and the anisotropic contributions can be extracted to restrain molecular geometry. The VASS technique can be widely applied to study both liquid crystals themselves (Grishtein et al., 2001) as well as biomolecules oriented within such

Submitted July 8, 2003, and accepted for publication September 8, 2003.

Address reprint requests to James H. Prestegard, E-mail: jpresteg@ccrc.uga.edu.

0006-3495/03/12/3848/10 $2.00

systems without the demands of conventional solid-state experiments. Fast spinning rates, typical of solid-state experiments, are not required to average anisotropy; rapid axially symmetric motion of a molecule oriented in a liquid crystal reduces effective chemical shift anisotropies (CSAs) and dipolar couplings by more than an order of magnitude such that slow spinning speeds (300–3000 Hz) and low decoupling powers can be employed. VASS has previously been demonstrated to scale the CSA in a small organic molecule (Vaananen et al., 1987) and to determine the sign of dipolar couplings in a peptide (Tian et al., 1999). A recent extension employs two-dimensional switched angle spinning. This technique requires a rapid change in sample orientation with respect to the magnetic field during the experiment; the resulting 2D data has been used to correlate anisotropic contributions to spectra with isotropic resonance positions (Havlin et al., 2003) and to obtain structural information on a peptide oriented in a lipid bilayer (Zandomeneghi et al., 2003b). In this article, we simply map resonance positions as a function of spinning angle to assign the multiple phosphorus resonances in strongly oriented phosphatidylinositol phosphates and to determine the anisotropic offsets to the chemical shift that can be used to restrict headgroup orientations with respect to the membrane surface.

Phosphatidylinositol phosphates, or phosphatidylinositides, occur at low levels in many biological membranes where they serve as second messengers in the regulation of a wide variety of cellular processes. More recently, their role in recruiting proteins to the membrane, in particular those with pleckstrin homology (PH) domains (Lemmon and Ferguson, 2000), has been investigated. There is also an interesting hypothesis involving the activation of ADP Ribosylation Factor 1 (ARF1) at the membrane surface. ARF1, a ubiquitous 20-kDa eukaryotic protein involved in membrane trafficking, uses its N-terminal myristoyl group to transiently associate with the cell membrane. It has been suggested that ARF1 specifically interacts with the headgroup of phosphatidylinositol bisphosphate ($PI(4,5)P_2$) (Terui et al., 1994), the major polyphosphatidylinositide found in mammalian cells (McLaughlin et al., 2002). With its large negative charge and specific phosphorylation sites, $PI(4,5)P_2$ may help recruit ARF1 to the membrane. Knowing phosphatidylinositide headgroup geometry at the membrane surface may help explain exactly how these proteins are targeted to the membrane. Here we use a combination of experimental and computational methods to illustrate how chemical shift offsets obtained from VASS provide orientational restraints on two specific phosphatidylinositides, phosphtidylinositol-4-phosphate (PI(4)P) and $PI(4,5)P_2$ embedded in a membrane-like bilayer.

THEORY

It is important to understand the connection between anisotropic contributions to phosphorus chemical shifts and molecular geometry constraints. The chemical shift of phosphate esters varies with orientation in a magnetic field due to the anisotropy of the group's electronic distribution; this gives rise to a chemical shift anisotropy contribution. If the group tumbles rapidly and samples orientations uniformly, shifts are averaged to the positions observed for resonances in high-resolution solution NMR, δ_{iso}. If the group has a preferred orientation, as it would when anchored to an oriented array of membrane mimetics, resonances are offset by an anisotropic contribution to isotropic chemical shifts, $\Delta\delta_{aniso}$. These offsets are measurable and can be used to place constraints on geometries of molecular models. For the case of an ordered array of bilayer fragments, $\Delta\delta_{aniso}$ can be expressed as

$$\begin{aligned}\Delta\delta_{aniso} &= \delta_{oriented} - \delta_{isotropic} \\ &= 1/3\, S_{bilayer}\{(\langle 3\cos^2\theta_1 - 1\rangle) \times (\delta_{11} - \delta_{22}) \\ &\quad + (\langle 3\cos^2\theta_3 - 1\rangle) \times (\delta_{33} - \delta_{22})\}, \end{aligned} \quad (1)$$

where $S_{bilayer}$ is the order parameter of the bilayer (which includes a factor of $-1/2$ when the bilayer normal is perpendicular to the liquid crystal director axis), δ_{nn} are the principal values of the static chemical shift tensor, θ_n are the angles between the bilayer normal and the principal axes of the chemical shift tensor, and the brackets account for additional averaging due to molecular motion. When shift tensors are axially symmetric, these equations become identical to those relating dipolar couplings to molecular geometry, and procedures similar to those for extracting geometrical information from dipolar couplings can be used to analyze conformational constraints from anisotropic contributions to the chemical shift. The values of δ_{nn} are well defined in a frame oriented in an individual phosphate ester group. The values and directions of principal axes can, therefore, be taken from suitable model compounds (Seelig, 1978). The angles θ_n of these axes relative to the magnetic field actually depend on molecular geometry through the way in which each phosphate is oriented: first, by the phosphate's connection to the inositol ring, second, by the way the ring is oriented in its connection to a diacylglycerol moiety, and third, by the way this moiety is inserted into the membrane. Orientations for phosphate groups allowed by particular molecular geometry can be used to calculate shift offsets, $\Delta\delta_{aniso}$, and these can be compared to experimental values to eliminate disallowed geometries.

For chemical shift anisotropy data, there is a complication in extracting $\Delta\delta_{aniso}$ from experimental data. This arises because $\Delta\delta_{aniso}$ often dominates resonance positions making it difficult to assign resonances to particular phosphate groups. One way to separate $\Delta\delta_{aniso}$ and δ_{iso} is to apply VASS to a molecule oriented through its interaction with a liquid crystal. VASS exploits the ability to redefine the direction of principal order relative to the magnetic field by spinning a liquid crystal at particular angles relative to the field (Courtieu et al., 1982).

Liquid crystals have been used extensively as solvents in which to determine the CSA of dissolved solute molecules (Lounila and Jokisaari, 1982). Static liquid crystals orient in a magnetic field depending on the anisotropy in magnetic susceptibility of a liquid crystal domain, $\Delta\chi$. In VASS the spinning rate must be fast enough to prevent reorientation of liquid crystal directors during rotation and slow enough to prevent centrifugation of sample. When spinning, the liquid crystal director orients to balance the magnetic and viscous torques on the liquid crystal, ideally aligning either parallel or perpendicular to the spinning axis, depending on the sign of $\Delta\chi$ and the angle the sample makes with respect to the magnetic field (Courtieu et al., 1982).

The chemical shift offset under VASS now becomes, in addition, a function of the angle of the spinning axis with respect to the magnetic field, β, as seen in Eqs. 2 and 3. Contributions to spectra are slightly different depending on whether the liquid crystal director is parallel or perpendicular to the spinning axis (Courtieu et al., 1994). When the angle β is less than the magic angle and $\Delta\chi < 0$, or β is more than the magic angle and $\Delta\chi > 0$, the anisotropy is scaled by an additional factor of $-1/2$.

$$\Delta\chi > 0\text{: } 0^\circ < \beta < 54.7^\circ$$

$$\Delta\chi < 0\text{: } 54.7^\circ < \beta < 90^\circ$$

$$\delta_{exp} = \delta_{iso} + \tfrac{1}{2}(3\cos^2\beta - 1)\,\Delta\delta_{aniso} \quad (2)$$

$$\Delta\chi > 0\text{: } 54.7^\circ < \beta < 90^\circ$$

$$\Delta\chi < 0\text{: } 0^\circ < \beta < 54.7^\circ$$

$$\delta_{exp} = \delta_{iso} - \tfrac{1}{4}(3\cos^2\beta - 1)\,\Delta\delta_{aniso}. \quad (3)$$

In our case we use a liquid crystal of negative anisotropy of susceptibility, or $\Delta\chi < 0$, and the liquid crystal director ''flips'' orientation from being parallel to perpendicular to the spinning axis upon moving from angles greater than the magic angle to angles less than the magic angle (Courtieu et al., 1982). From these equations it is clear that a plot of δ_{exp} versus $(3\cos^2\beta - 1)$ can be used to separate δ_{iso} and $\Delta\delta_{aniso}$.

MATERIALS AND METHODS

Sample preparation

A number of phospholipid-based liquid crystalline systems exist for orienting biomolecules. For the phosphatidylinositides studied in this preliminary application of the VASS technique, we chose a bilayered liquid crystal (Freyssingeas et al., 1996; Gaemers and Bax, 2001; Jonstromer and Strey, 1992) with no phosphorus atoms to reduce problems with background ^{31}P signals. When combined in specific ratios with *n*-alcohols, aqueous solutions of poly(ethylene) glycol ethers form bilayers that align in a magnetic field (Jonstromer and Strey, 1992; Ruckert and Otting, 2000). These bilayer systems have a negative anisotropy of susceptibility and orient with their normal perpendicular to the field. Homogenous orientations of a liquid crystalline phase composed of 17.7% (w/w) pentaethylene glycol monododecyl ether (C12E5) and 5.2% hexanol ($r = 0.87$, where r is the molar ratio of poly(ethylene)glycol:alcohol) in water and of a similar liquid crystalline phase composed of 17.1% (w/w) pentaethylene glycol octyl ether (C8E5) and 5.5% (w/w) octanol in water ($r = 1.17$) were found to occur in the temperature range from 21 to 28°C. All chemicals were purchased from Sigma (Sigma-Aldrich, St. Louis, MO) and used without further purification. Pure PI(4)P and PI(4,5)P_2 (both from Avanti Polar Lipids, Alabaster, AL) were dried under a stream of nitrogen and dispersed into the bilayers in low molar ratios (where PIP:C_nE_m is 1:100–1:200) so that interactions between phosphatidylinositide molecules would be weak and the bilayer order would not be disrupted.

Instrumentation

^{31}P VASS spectra were collected at 202.6 MHz on a 500-MHz Varian Inova spectrometer using a Doty Scientific XC5 VASS probe (Doty Scientific, Columbia, SC) at several angles (90°–20°) of the spinning axis relative to the magnetic field. The angle was adjusted to within 2° of the indicated angle by starting from the magic angle (determined using KBr) and adjusting the angle-controlling dial on the probe, previously calibrated to give a change in 10° for one rotation of the dial. The ^{31}P 90° pulse length varied from 7 μs at large angles to 12 μs at small angles as expected for the probe's solenoid coil. Waltz ^{1}H decoupling was applied during acquisition. The recycle time was 2.0 s, and the number of scans varied for each angle from 1000 to 12000 depending on the signal/noise ratio at a given angle. Spinning speeds from 300 to 3000 Hz were used, and the spinning rate was controlled to within 2 Hz by a spin rate Probe Controller (Doty Scientific). Initially ^{31}P chemical shifts were measured relative to an internal signal from 10 mM inorganic phosphate (pH 7.4) and then referenced to 85% phosphoric acid by subtracting 1.579 ppm. The strong ^{31}P signal from inorganic phosphate occasionally obscured resonances from the phosphomonoesters, making assignment difficult in some samples. A nonphosphate buffer (10mM TES, 50mM NaCl, 10% D_2O, pH 7.2) aided in assignment of resonances in these samples. Samples without inorganic phosphate were referenced indirectly by correlating the water resonance frequency in these samples to that in a phosphate-containing sample examined immediately before and after the ^{31}P observation (Maurer and Kalbitzer, 1996). The degree of sample ordering and homogeneity was monitored through ^{2}H quadrupolar splittings from 10% D_2O added to all samples using the VASS probe tuned to ^{2}H (76.8 MHz).

Chemical shift offset analysis

To aid in the analysis of experimental data, chemical shift offsets for the phosphomonoesters and diesters were calculated for models of both PI(4)P and PI(4,5)P_2. Energy-minimized models were rotated about a pair of torsion angles ($\alpha 1$ and $\alpha 1'$) as defined in Fig. 1 in steps of 10°. For each model produced in this systematic conformational search, chemical shift offsets were calculated. This calculation relies on the successive transformation of the phosphate chemical shift tensor in its principal axis frame first to the local phosphatidylinositide molecular frame, second to an axially averaged bilayer normal frame, and third to the laboratory frame. To eliminate $S_{bilayer}$ and any additional axially symmetric averaging, monoester shifts were scaled relative to the diester shift at each point. A program was written in Maple (Maple 7.0, Waterloo Maple, Waterloo, Canada) to carry out these transformations and to calculate chemical shifts.

The root mean square deviation (rmsd) between the calculated chemical shift offsets and the experimentally observed chemical shift offsets was calculated at each combination of angles and for each phosphate ester under consideration. Structures having rmsd values within estimates of experiment were filtered through steric constraints imposed at normal van der Waals radii. To accomplish this filtering, a systematic conformational search of the phosphatidylinositide structures about selected torsion angles was performed in the molecular modeling program Sybyl (Sybyl 6.7, Tripos, St. Louis, MO), and conformations generated with significant van der Waals

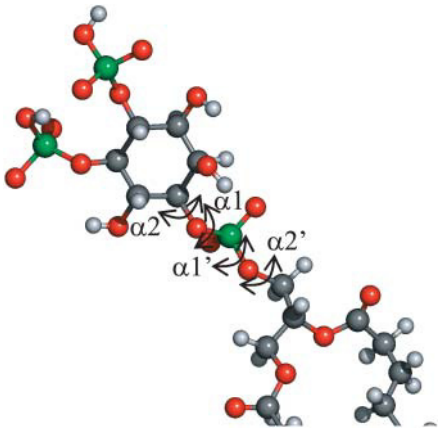

FIGURE 1 PI(4,5)P_2 showing the dihedral angles of greatest variability. (Acyl chains have been truncated.)

radii overlap were eliminated. Typically in these calculations electrostatic terms were turned off, and an energy cutoff of 5 kcal/mol over the minimal conformationally dependent energy was used.

RESULTS

The stacked plot in Fig. 2 shows ^{31}P NMR spectra of PI(4)P (Fig. 2 *A*) and PI(4,5)P_2 (Fig. 2 *B*) collected at different spinning angles with respect to the magnetic field; it illustrates how VASS systematically scales the chemical shift offset. One of the first tasks was to assign the resonances to various phosphate sites. This cannot usually be done directly from spectra dominated by anisotropic offsets because they are highly geometry-dependent and can obscure the purely chemical information dominating isotropic shift values. Extrapolation of anisotropic offsets to their isotropic shifts using VASS makes their assignment easier. For PI(4)P and PI(4,5)P_2 the difference between the phosphodiester and phosphomonoester signals, both in isotropic and oriented spectra, is large enough to allow the assignment of the upfield shifted resonance to the diester by analogy to other phosphodiesters (Tebby, 1991). In Fig. 2, the diester peak is labeled D. In PI(4,5)P_2, distinguishing the two monoesters is more difficult. In detergent micelles, their isotropic chemical shifts are distinct due to their different degrees of ionization at the pH of observation (van Paridon et al., 1986). Their assignment is given in Fig. 2 *B*, *d*, the analogous isotropic magic angle spectrum, and this is denoted by the labels M4 and M5 for monoester 4 or 5. In the oriented bilayers, separation in chemical shifts for these two resonances persisted at all angles, but if we were limited to data at only one angle, we could not assume assignments would fall in the same order; the movement of both resonances from 36° to 54.7° or 54.7° to 90° is, in fact, larger than their chemical shift difference, and an exchange of positions is possible. Following the movement as a function of angle allows an unambiguous assignment as indicated in Fig. 2. The large ^{31}P signal in all spectra is due to

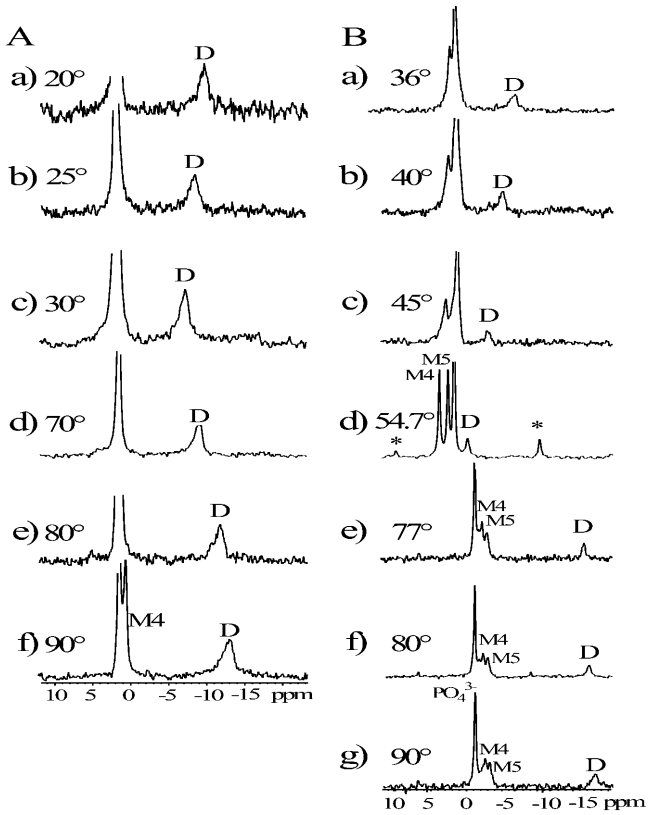

FIGURE 2 ^{31}P spectra of (*A*) PI(4)P oriented in 17% (w/w) C12E5/*n*-hexanol (5.5%, w/w, 1:200, PI(4)P, C12E5) at 25°C ± 1 at 2000-Hz spinning rate. Phosphomonoester and diester peaks are indicated in the figure and readily identifiable by their distinctive chemical shifts. Spinning sidebands are marked by asterisks. Each spectrum was collected at the angle indicated in the figure. (*B*) PI(4,5)P_2 oriented in 17% (w/w) C12E5/*n*-hexanol (5.5%, w/w, 1:200, PI(4,5)P_2, C12E5) at 24°C ± 1. Spectra *a–d* were collected at a spinning rate of 2000 Hz, and spectra *e–g* were collected at an 800 Hz spinning rate.

phosphate buffer at pH 7.4. This signal provided a chemical shift reference in oriented spectra, but occasionally obscured the monophosphates' signals. In these cases, a phosphate-free buffer at pH 7.2 was used.

Spectra recorded at angles less than 54.7° (Fig. 2, *A*, *a–c*, and *B*, *a–c*) showed lower signal/noise due to the angle of the field relative to the axis of the solenoid coil built into the VASS stator. At these angles the liquid crystal director is oriented perpendicular to the spinning axis and modulation of chemical shift by spinning can further degrade signals. Some loss of signal could also be the result of a mosaic spread of the director orientation (Tian et al., 1999; Zandomeneghi et al., 2003b) and the associated appearance of a partial powder pattern; this spread and the appearance of weak sidebands observed at lower spinning rates compromise spectral quality. Significant sidebands also appear when the sample spinning axis is close to the magic angle (54.7° ± 10.0°) due to the disordering of liquid crystal domains; sidebands to the diester peak are shown with an asterisk (*)

in Fig. 2 *B*, *d*. Most data points were collected at higher spinning rates and away from the magic angle to avoid effects of disorder. It is interesting to note that the direction of shift, as a function of angle, changes at the magic angle. The diester peak, for example, moves upfield with decreasing angle in the range 0–54.7° but downfield with decreasing angle in the range 54.7°–90°. This is a result of a change in liquid crystal director axis from parallel to the spinning axis above 54.7° to perpendicular to the axis below 54.7°.

The predicted angular dependence given in Eqs. 2 and 3 can be used to systematically correlate observed chemical shifts to their isotropic shifts. Fig. 3 shows the linear dependence of the chemical shift on the scaling factor ($3\cos^2\beta - 1$). Using Eqs. 2 and 3, the isotropic chemical shifts and chemical shift offsets were evaluated by a least squares fit to the data for PI(4)P and PI(4,5)P_2. The extrapolated isotropic chemical shifts calculated from VASS data agree very well within estimated error to the isotropic shifts obtained from magic angle experiments (spinning at 54.7°) or micellar solution as indicated in Table 1. However, the angular dependence of chemical shift offsets is not always as simple as depicted in Fig. 3. It has been noted that liquid crystal director alignment can deviate from ideal behavior at certain spinning rates (Bayle et al., 1988; Vivekanandan et al., 2002). In particular, at spinning rates other than those used here, the flip of the director can occur at angles other than the magic angle, and at very fast spinning rates the director may not change direction at all due to centrifugal torque. At the spinning rates employed in this study (300–3000 Hz), we observed the director flipping from one side to the other very near the magic angle. However, extrapolated isotropic chemical shifts from the low side of the magic angle did not always agree with chemical shifts from the high side of the magic angle or isotropic chemical shifts observed in micellar spectra. The point at which the theoretical curves for extrapolating isotropic chemical shifts cross in Fig. 3 is at an angle ~4° off the magic angle. This small uncertainty could be mechanical in origin, due to error in the calibration of the angle, or it could result from this more complicated behavior of the liquid crystal director axis. Additional effects also appeared at lower spinning rates. At the spinning rates given in Fig. 2, both the diester and monoester peaks were well resolved, showed minimal spinning sidebands, and yielded acceptable, extrapolated isotropic chemical shifts.

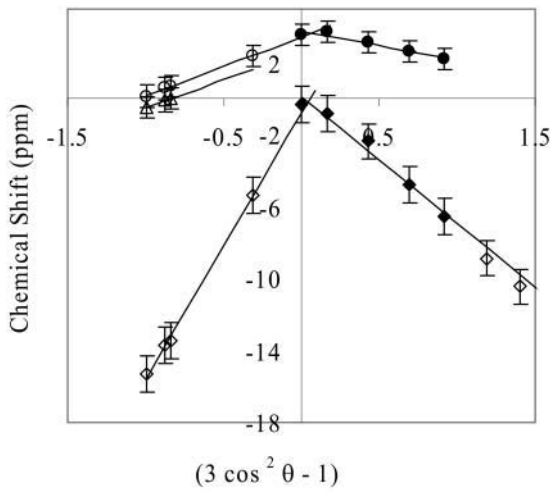

FIGURE 3 ^{31}P chemical shifts as a function of ($3\cos^2\beta - 1$). Isotropic chemical shifts of the phosphorus atoms were calculated from the chemical shift offsets by extrapolating their linear dependence on ($3\cos^2\beta - 1$) to their magic angle. ○ represents the monoester-4 at 800 Hz, ● represents the monoester-4 at 2000 Hz, △ represents the monoester-5 at 800 Hz, ◇ represents the diester at 800 Hz, and ♦ represents the diester at 2000 Hz.

DISCUSSION

The limited number of restraints available from the data in Table 1 (two $\Delta\delta_{aniso}$ from PI(4)P and three $\Delta\delta_{aniso}$ from PI(4,5)P_2), precludes a direct extraction of molecular geometry. Experimental chemical shift offsets were therefore compared to calculated chemical shift offsets that could be observed, given reasonable geometry restrictions, for a phosphatidylinositide inserted into a membrane. We chose to model the phosphatidylinositides and apply normal van der Waals radius constraints to limit the number of possible solutions to headgroup geometry. We then calculated the chemical shift offsets as a function of a small set of rotatable torsion angles. Molecular modeling programs were used to construct molecules with an appropriate starting geometry. First, models of PI(4)P and PI(4,5)P_2 were generated and minimized in Sybyl and found to yield the idealized phosphatidylinositol geometry: $\alpha2' = 180°$, $\alpha1' = 180°$, $\alpha1 = 180°$, and $\alpha2 = -60°$ (Bradshaw et al., 1999). Electrostatic charges, both partial and formal, were set to zero in this minimization to eliminate problems that could stem from poor representation of electrostatics in these amphiphilic, membrane-associating molecules. From the starting model described above, a series of molecular models for molecular orientations of the headgroup was generated by performing a systematic conformational search about the three dihedral angles connecting the headgroup to the bilayer: $\alpha1$, $\alpha1'$, and $\alpha2$ shown in Fig. 1. $\alpha2'$ was assumed to be rigid based on a lack of variation in model phospholipids, and its value (180°) was fixed based on the suggested ideal orientation of PI(4)P in a membrane bilayer (Bradshaw et al., 1999). Other torsion angles of the phosphatidylinositide are likely to be severely restricted due to burial in the bilayer. The search produced a number of possible conformations based on allowable van der Waals contacts. Here we applied a cut-off energy of ~5 kcal/mol above the minimal energy structure to select a set of sterically allowed conformations.

For the chemical shift offset calculations, another series of models consistent with Sybyl geometry was generated. First, inositol phosphate models of the headgroups were built

TABLE 1 Chemical shift offsets and isotropic chemical shifts of phosphatidylinositides

Phosphate group	Calculated δ_{iso} (ppm)*	Observed δ_{iso} (ppm)†	Observed δ_{iso} (ppm)‡	Calculated $\Delta\delta_{aniso}$ (ppm)§	Calculated $\Delta\delta_{aniso}$ (ppm)¶
PI(4,5)P_2 (monoester-4)	3.5 ± 0.3	3.6 ± 0.1	3.5 ± 0.1	6.8 ± 0.1	8.2 ± 0.2
PI(4,5)P_2 (monoester-5)	2.3 ± 0.1	2.4 ± 0.1	2.4 ± 0.1	5.3 ± 0.5	–
PI(4,5)P_2 (diester)	−0.9 ± 0.4	−0.3 ± 0.1	−0.4 ± 0.1	29.0 ± 0.5	25.4 ± 0.6
PI(4)P (monoester)	3.3 ± 0.1	3.5 ± 0.1	–	5.5 ± 0.1	4.9 ± 0.1
PI(4)P (diester)	−0.3 ± 0.2	–	–	28.3 ± 0.1	–

Errors given for δ_{iso} and $\Delta\delta_{aniso}$ are standard deviations from a least squares fit of the data to a linear equation; other errors reported are experimental errors estimated from spectral resolution.

*Isotropic chemical shift calculated from VASS data.

†Isotropic chemical shift observed from magic angle spinning spectrum.

‡Isotropic chemical shift observed from micellar solution.

§VASS-calculated CSA for ($\beta > \beta_m$), where β is the angle the sample makes with the magnetic field and β_m is the magic angle.

¶VASS-calculated CSA for ($\beta < \beta_m$).

using the MM2 package in Chem3D (CambridgeSoft Corporation 4.0, Cambridge, MA). Comparison to experimentally determined inositol phosphate crystal structures revealed that the gas phase MM2 force field did not distort the geometry of inositol phosphates significantly (Spiers et al., 1995). Though all bonds may experience some degree of flexibility, those in the headgroup ring can certainly be assumed to be rigid. The inositol phosphate models were added to one of the diacylglycerol conformers found in the unit cell of dimyristoylphosphatidylcholine (DMPC) (Pearson and Pascher, 1979) to produce the same starting geometry as in the Sybyl structures.

Calculations of chemical shift offsets for each of the models proceeded by first assigning CSA tensors to each phosphate. The principal values of the phosphodiester chemical shift tensor were taken from single crystal, solid-state NMR studies of dipalmitoylphosphatidylcholine (DPPC) (Herzfeld et al., 1978), and elements of the static monoester chemical shift tensor were taken from serine phosphate (Kohler and Klein, 1977b). In the case of the monoesters, chemical shift tensors were made axially symmetric to mimic rotation about the O–P ester bonds. Chemical shift offsets were then calculated for all models by applying a series of coordinate transformations from the phosphate principal axis frame into the laboratory frame. The time-averaged orientations of the acyl chains are assumed parallel to the bilayer normal, consistent with previous assumptions of membrane-associating species (Howard and Prestegard, 1995).

Calculated chemical shift offsets for each phosphate group in all headgroup orientations were compared to the VASS-determined chemical shift offsets. Since $S_{bilayer}$ in Eq. 1 is not known for the liquid crystals used in these experiments, the ratio of the calculated monoester to calculated diester chemical shift offset for each orientation was compared to the ratio of the experimentally observed monoester to experimentally observed diester chemical shift offset. Root mean square deviation between calculated and observed chemical shift offsets for the monoesters below an estimated error of 5 ppm was used to restrict possible headgroup geometries. This error limit is larger than experimental error (~1 ppm), and larger than propagated experimental errors from static model compound tensors (Kohler and Klein, 1977a); it is meant to account for some uncertainty in selection of proper model compounds.

Because calculating chemical shift offsets as a function of multiple torsion angles becomes computationally expensive, we chose to first restrict $\alpha 2$ to one of several representative geometries allowed by van der Waals constraints. The Sybyl systematic conformational search for van der Waals restraints with an energy spread of 5 kcal/mol above the minimal energy conformation yielded a bimodal distribution of $\alpha 2$ values for PI(4)P centered around $-80 \pm 15°$ and $-145 \pm 15°$ (data not shown). A similar distribution of $\alpha 2$ values for PI(4,5)P_2 was also obtained. These values of $\alpha 2$ were used in chemical shift calculations for both PI(4)P and PI(4,5)P_2. Points with root mean square deviation between the calculated and observed chemical shift offsets less than 5 ppm are shown for PI(4)P with $\alpha 2 = -80°$ in Fig. 4. No geometries were allowed within the 5.0-ppm rmsd cutoff for $\alpha 2 = -145°$. The allowed geometries shown in Fig. 4 fall into three families of possible orientations. These are dispersed in conformational space and the angular ranges

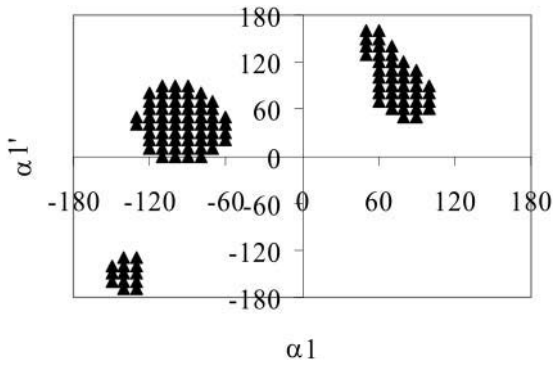

FIGURE 4 PI(4)P conformers as a function of $\alpha 1$ and $\alpha 1'$ for fixed $\alpha 2 = -80°$ having a root mean square error difference between calculated and observed chemical shift offsets of 5.0 ppm or less. Points have not been filtered by applying van der Waals constraints.

in two of the families are broad due to the small number of experimental constraints. For PI(4,5)P_2 chemical shift calculations as a function of $\alpha1$ and $\alpha1'$ at $\alpha2$ values of $-80°$ and $-145°$ and are shown in Fig. 5, *a* and *b*, respectively. The geometries allowed based on chemical shift offset observation (within a 5.0-ppm cutoff) are equally broad in the case of $\alpha2 = -145°$ (Fig. 5 *b*), but more restrained in the case of $\alpha2 = -80°$ (Fig. 5 *a*). The latter is in line with the existence of more experimental restraints for the bisphosphate.

Filtering the structures allowed by chemical shift offset data through results from Sybyl energy calculations further restricted geometries and allowed a more precise determination of orientation. Fig. 6 shows the results of filtering chemical shift offsets allowed for PI(4)P and PI(4,5)P_2 structures through the steric filter provided by a 5-kcal/mol energy cutoff in Sybyl. For PI(4)P (Fig. 6 *a*) there are significant reductions in allowed conformational space, but several distinctly different $\alpha1$, $\alpha1'$ combinations remain. For PI(4,5)P_2, there are also reductions in allowed conformational space for both $\alpha2 = -80°$ (Fig. 6 *b*) and $\alpha2 = -145°$ (Fig. 6 *c*), and only a few well-defined combinations of $\alpha1$ and $\alpha1'$ remain.

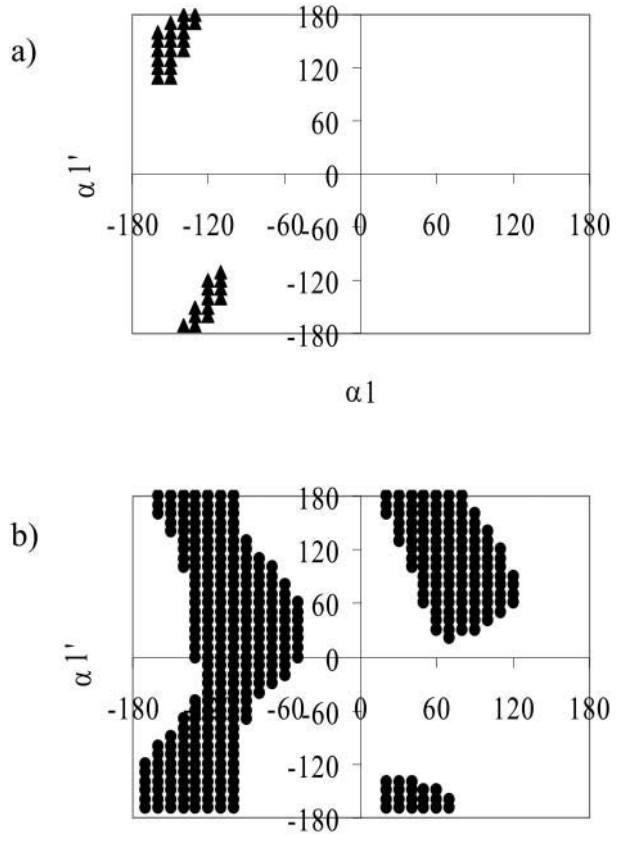

FIGURE 5 PI(4,5)P_2 conformers as a function of $\alpha1$ and $\alpha1'$ having a root mean square error difference between calculated and observed chemical shift offsets of 5.0 ppm or less. (*a*) Fixing $\alpha2 = -80°$ and (*b*) fixing $\alpha2 = -145°$.

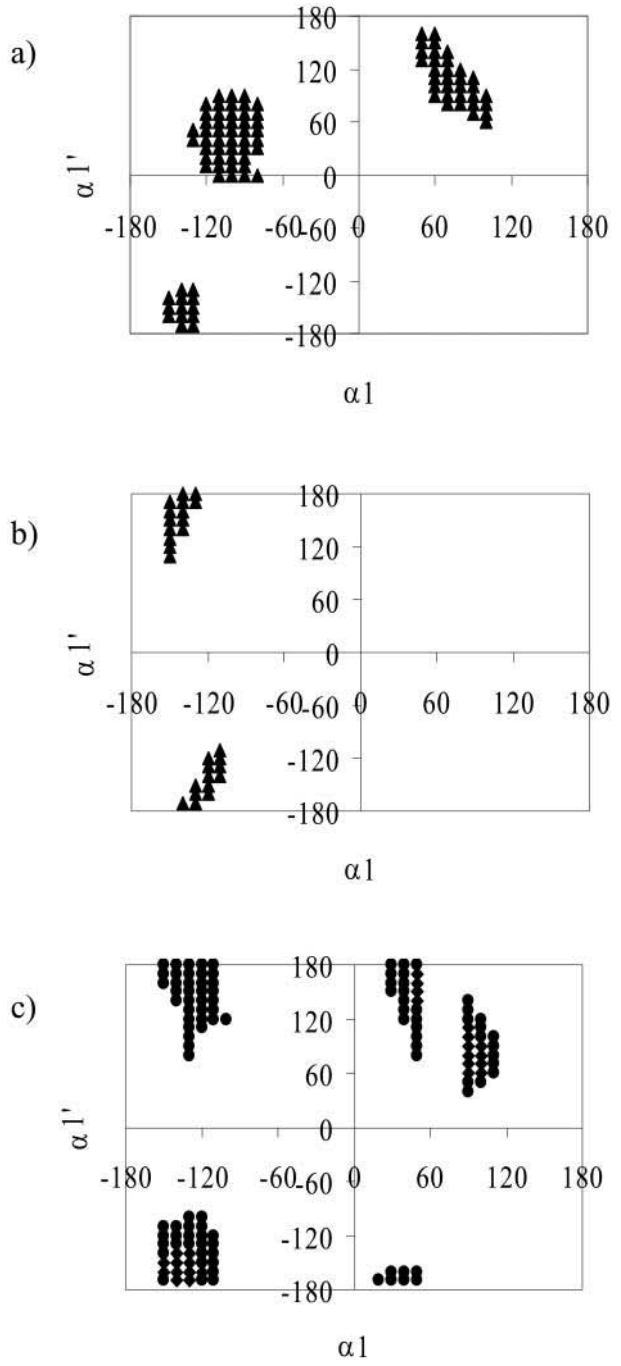

FIGURE 6 Allowed conformers after filtering through van der Waals constraints. (*a*) PI(4)P conformers with rmsd of 5.0 ppm or less are shown as a function of rotating $\alpha1$ and $\alpha1'$ with $\alpha2 = -80°$. (*b*) PI(4,5)P_2 conformers with rmsd of 5.0 ppm or less are shown as a function of rotating $\alpha1$ and $\alpha1'$ with $\alpha2 = -80°$ and (*c*) PI(4,5)P_2 conformers with rmsd of 5.0 ppm or less are shown as a function of rotating $\alpha1$ and $\alpha1'$ with $\alpha2 = -145°$.

It is clear from the range of allowed solutions in Figs. 4–6 that we cannot define a unique orientation for either PI(4)P or PI(4,5)P_2. However, Figs. 7 and 8 show some representative structures of these phosphatidylinositides. In each case, the structure represents the point with the lowest rmsd of

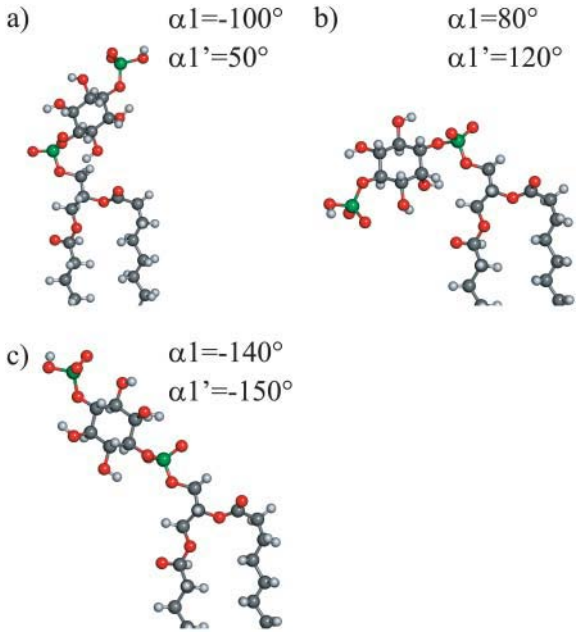

FIGURE 7 Possible conformations of PI(4)P in a bilayer. Dihedral angles $\alpha 1$ and $\alpha 1'$ are indicated ($\alpha 2 = -80°$). (All figures were prepared using PyMol (DeLano, 2002).)

chemical shifts within a given family and angles differs by no more than 20° from any member of the family. Three possible structures for PI(4)P are shown in Fig. 7. The energy difference between any two of the structures is no more than 1.3 kcal/mol. The orientation of the PI(4)P headgroup varies substantially as expected for the limited number of restraints in this molecule. Molecular geometries for PI(4,5)P_2 are better defined as seen in Fig. 8. The structures of PI(4,5)P_2 in Fig. 8 feature the inositol phosphate ring bent toward the bilayer surface. The structure in Fig. 8 *d* differs from those in Fig. 8, *a–c*, by ~1 kcal/mol more in energy.

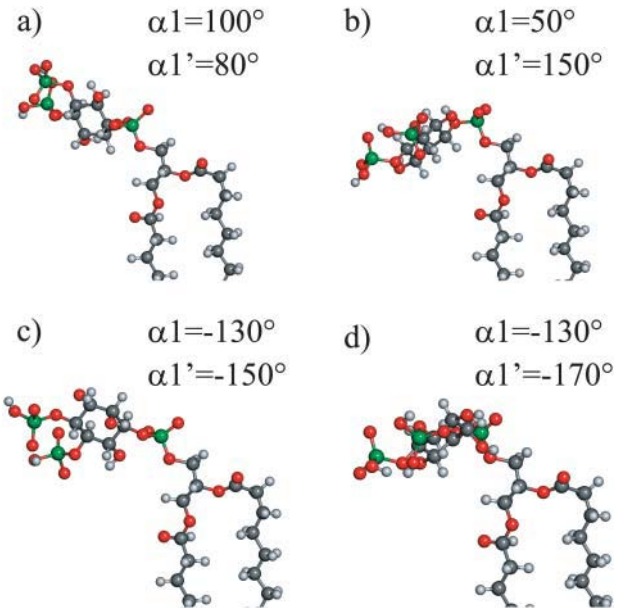

FIGURE 8 Possible conformations of PI(4,5)P_2 in a bilayer. *a–c* for $\alpha 2 = -145°$ and *d* for $\alpha 2 = -80°$. Dihedral angles $\alpha 1$ and $\alpha 1'$ are indicated.

Previous studies of specifically deuterated phosphatidylinositides oriented in dimyristoylphosphatidylcholine model membranes postulated that the unphosphorylated inositol ring sits nearly perpendicular to the membrane surface to maximize hydrogen bonds with solvent (Bradshaw et al., 1999), and upon phosphorylation, the ring bends toward the membrane as a result of electrostatic interactions with the positively charged choline headgroups (Bradshaw et al., 1996, 1997; Bushby et al., 1990; Hansbro et al., 1992). Our findings on orientation for the PI(4)P headgroup geometry do encompass previously proposed structures (Bradshaw et al., 1997) and do show headgroups with more extended conformations. The structure in Fig. 7 *b* is probably unreasonable in that it would partially bury the headgroup in the bilayer surface.

We believe our study provides the first experimental report of possible PI(4,5)P_2 headgroup geometries. In all cases, there is a pronounced tendency for the inositol phosphate ring to bend toward the membrane surface. This cannot arise from specific electrostatic interactions with choline in our case, because we are using bilayers made from neutral alkyl-poly(ethylene)glycol and long-chain alcohols. These interactions may result from more subtle effects such as specific water- or alcohol-mediated hydrogen bonding that dictates these preferences in our case. In any event, knowing something about the preferred headgroup geometry of phosphatidylinositides could greatly assist in understanding the specific interactions between phosphatidylinositides and the proteins that bind them. This study represents a first step in this direction.

We, unfortunately, cannot be too definitive in our discussion of molecular geometry implications. There are a number of important assumptions underlying the work we have presented. Use of phosphorus chemical shift tensors from model compounds in calculations on more complex systems such as the phosphatidylinositides introduces significant error in the calculation of chemical shift offsets. It is also important to note that we have made assumptions about the lack of internal motion to simplify the analysis of chemical shift offset data. Chemical shift offset restraints can only reflect the average orientation of one tensor relative to another, and structures generated are virtual structures in cases where substantial internal motion exists. Finally, the model membrane we have used is far from a true biological membrane in its surface character.

More important than specific information on a set of membrane lipids is the fact that we have illustrated the utility of some important methodology. Using PI(4,5)P_2 we have shown the feasibility of chemical shift assignments and extraction of chemical shift offsets using VASS. The high natural abundance of ^{31}P and the large chemical shift

difference between the monoesters and diester made this technique easy to use on these phospholipids. However, the use of the linear dependence of chemical shift on angle helped in assigning poorly resolved monoester peaks. In more complicated spectra, this technique may become very important. There are also ways of improving geometry definition and relaxing underlying assumptions. Isotopic labeling of strongly oriented biomolecules will provide more data and better definition of geometries, and we may also be able to introduce specific models for internal motion. For lipids, introduction and observation of ^{13}C would avoid difficulties with phosphorus background in phospholipid-based membrane preparations. Chemical shift restraints from groups with large chemical shift anisotropies such as ^{13}C labeled carbonyl groups should prove particularly valuable. For proteins, ^{13}C and ^{15}N introduction and observation would provide a wealth of information. However, the separation of chemical shift offsets and assignment of 100 or more peaks in a strongly oriented protein spectrum can be a major task. VASS may be particularly advantageous here. Hence, we believe the work we have presented points to some bright prospects for the future.

The authors thank Dr. John Glushka and Denny Warrenfeltz for technical assistance and Dr. Junfeng Wang, Dr. Catherine Bougault, Ronald Seidel, Dr. Juan Carlos Amor, and Prof. Richard Kahn for valuable discussions.

This work is supported by a grant from the National Institutes of Health (GM61268).

REFERENCES

Almeida, F. C. L., and S. J. Opella. 1997. Fd coat protein structure in membrane environments: structural dynamics of the loop between the hydrophobic trans-membrane helix and the amphipathic in-plane helix. *J. Mol. Biol.* 270:481–495.

Arora, A., F. Abildgaard, J. H. Bushweller, and L. K. Tamm. 2001. Structure of outer membrane protein A transmembrane domain by NMR spectroscopy. *Nat. Struct. Biol.* 8:334–338.

Bayle, J. P., F. Perez, and J. Courtieu. 1988. Inertial effects in rotating lyotropic liquid crystals. *Liquid Crystals.* 3:753–758.

Bradshaw, J. P., R. J. Bushby, C. C. D. Giles, and M. R. Saunders. 1999. Orientation of the headgroup of phosphatidylinositol in a model biomembrane as determined by neutron diffraction. *Biochemistry.* 38:8393–8401.

Bradshaw, J. P., R. J. Bushby, C. C. D. Giles, M. R. Saunders, and D. G. Reid. 1996. Neutron diffraction reveals the orientation of the headgroup of inositol lipids in model membranes. *Nat. Struct. Biol.* 3:125–127.

Bradshaw, J. P., R. J. Bushby, C. C. D. Giles, M. R. Saunders, and A. Saxena. 1997. The headgroup orientation of dimyristoylphosphatidylinositol-4-phosphate in mixed lipid bilayers: a neutron diffraction study. *Biochim. Biophys. Acta.* 1329:124–138.

Bushby, R. J., S. J. Byard, P. M. Hansbro, and D. G. Reid. 1990. The conformational behavior of phosphatidylinositol. *Biochim. Biophys. Acta.* 1044:231–236.

Chou, J., J. Kaufman, S. J. Stahl, P. Wingfield, and A. Bax. 2002. Micelle-induced curvature in a water-insoluble HIV-1 Env peptide revealed by NMR dipolar coupling measurement in stretched polyacrylamide gel. *J. Am. Chem. Soc.* 124:2450–2451.

Courtieu, J., D. W. Alderman, D. M. Grant, and J. P. Bayles. 1982. Director dynamics and NMR applications of nematic liquid crystals spinning at various angles from the magnetic field. *J. Chem. Phys.* 77:723–730.

Courtieu, J., J. P. Bayle, and B. M. Fung. 1994. Variable-angle sample-spinning NMR in liquid-crystals. *Prog. NMR Spectr.* 26:141–169.

DeLano, W. L. 2002. The PyMOL Molecular Graphics System. Delano Scientific, San Carlos, CA.

Fernandez, C., C. Hilty, S. Bonjour, K. Adeishvili, K. Pervushin, and K. Wuthrich. 2001. Solution NMR studies of the integral membrane proteins OmpX and OmpA from *E. coli*. *FEBS Lett.* 504:173–178.

Freyssingeas, E., F. Nallet, and D. Roux. 1996. Measurement of the membrane flexibility in lamellar and ''sponge'' phases of the C12E5/hexanol/water system. *Langmuir.* 12:6028–6035.

Gaemers, S., and A. Bax. 2001. Morphology of three lyotropic liquid crystalline biological NMR media studied by translational diffusion anisotropy. *J. Am. Chem. Soc.* 123:12343–12352.

Grishtein, J., D. McElheny, V. Frydman, and L. Frydman. 2001. A variable-director ^{13}C NMR analysis of lyotropic aramide solutions. *J. Chem. Phys.* 114:5415–5424.

Hansbro, P. M., S. J. Byard, R. J. Bushby, P. J. H. Turnbull, N. Boden, M. R. Saunders, R. Novelli, and D. G. Reid. 1992. The conformational behavior of phosphatidylinositol in model membranes—^{2}H NMR Studies. *Biochim. Biophys. Acta.* 1112:187–196.

Havlin, R. H., G. H. J. Park, T. Mazur, and A. Pines. 2003. Using switched angle spinning to simplify NMR spectra of strongly oriented samples. *J. Am. Chem. Soc.* 125:7998–8006.

Herzfeld, J., R. G. Griffin, and R. A. Haberkorn. 1978. Phosphorus-31 chemical shift tensors in barium diethyl phosphate and urea-phosphoric acid: model compounds for phospholipid head-group studies. *Biochemistry.* 17:2711–2718.

Howard, K. P., and J. H. Prestegard. 1995. Membrane and solution conformations of monogalactosyldiacylglycerol using NMR molecular modeling methods. *J. Am. Chem. Soc.* 117:5031–5040.

Jonstromer, M., and R. Strey. 1992. Nonionic bilayers in dilute solutions: effect of additives. *J. Phys. Chem.* 96:5993–6000.

Kohler, S. J., and M. P. Klein. 1977a. Orientation and dynamics of phospholipid head groups in bilayers and membranes determined from ^{31}P nuclear magnetic resonance chemical shielding tensors. *Biochemistry.* 16:519–526.

Kohler, S. J., and M. P. Klein. 1977b. Phosphorus-31 NMR chemical shielding tensors of L-O-serine phosphate and 3′-vytidine monophosphate. *J. Am. Chem. Soc.* 99:8290–8293.

Lemmon, M. A., and K. M. Ferguson. 2000. Signal-dependent membrane targeting by pleckstrin homology (PH) domains. *Biochem. J.* 350:1–18.

Lounila, J., and J. Jokisaari. 1982. Anisotropies in spin-spin coupling constants and chemical shifts as determined from the NMR spectra of molecules oriented by liquid crystal solvents. *Prog. NMR Spectr.* 15: 249–290.

Marassi, F., and S. J. Opella. 1998. NMR structural studies of membrane proteins. *Curr. Opin. Struct. Biol.* 8:640–648.

Marassi, F. M., and S. J. Opella. 2000. A solid-state NMR index of helical membrane protein structure and topology. *J. Magn. Reson.* 144:150–155.

Maurer, T., and H. R. Kalbitzer. 1996. Indirect referencing of ^{31}P and ^{19}F NMR Spectra. *J. Magn. Reson. Ser. B.* 113:177–178.

McLaughlin, S., J. Y. Wang, A. Gambhir, and D. Murray. 2002. PIP_2 and proteins: interactions, organization, and information flow. *Annu. Rev. Biophys. Biomol. Struct.* 31:151–175.

Patzelt, H., A. S. Ulrich, H. Egbringhoff, P. Dux, J. Ashurst, B. Simon, H. Oschkinat, and D. Oesterhelt. 1997. Towards structural investigations on isotope labeled native bacteriorhodopsin in detergent micelles by solution-state NMR spectroscopy. *J. Biomol. NMR.* 10:95–106.

Pauli, J., M. Baldus, B. van Rossum, H. J. M. de Groot, and H. Oschkinat. 2001. Backbone and side-chain ^{13}C and ^{15}N signal assignments of the α-spectrin SH3 domain by magic angle spinning solid-state NMR at 17.6 Tesla. *Chem. Biochem.* 2:272–281.

Pearson, R. H., and I. Pascher. 1979. The molecular structure of lecithin dihydrate. *Nature*. 281:499–501.

Rienstra, C. M., M. Hohwy, M. Hong, and R. G. Griffin. 2000. 2D and 3D N-15-C-13-C-13 NMR chemical shift correlation spectroscopy of solids: assignment of MAS spectra of peptides. *J. Am. Chem. Soc.* 122:10979–10990.

Rienstra, C. M., L. Tucker-Kellogg, C. P. Jaroniec, M. Hohwy, B. Reif, M. T. McMahon, B. Tidor, T. Lozano-Perez, and R. G. Griffin. 2002. *De novo* determination of peptide structure with solid-state magic-angle spinning NMR spectroscopy. *Proc. Natl. Acad. Sci. USA*. 99:10260–10265.

Ruckert, M., and G. Otting. 2000. Alignment of biological macromolecules in novel nonionic liquid crystalline media for NMR experiments. *J. Am. Chem. Soc.* 122:7793–7797.

Seelig, J. 1978. ^{31}P Nuclear magnetic resonance and the head group structure of phospholipids in membranes. *Biochim. Biophys. Acta*. 515:105–140.

Spiers, I. D., S. Freeman, and C. H. Schwalbe. 1995. Crystal structure and modeling studies of myo-inositol 1,2,3-trisphosphate. *J. Chem. Soc. Chem. Commun*. 21:2119–2120.

Tebby, J. C., editor. 1991. Handbook of Phosphorus-31 Nuclear Magnetic Resonance Data. CRC Press, Boca Raton, FL.

Terui, T., R. A. Kahn, and P. A. Randazzo. 1994. Effects of acid phospholipids on nucleotide exchange properties of ADP-Ribosylation Factor-1—evidence for specific interaction with phosphatidylinositol 4,5-bisphosphate. *J. Biol. Chem.* 269:28130–28135.

Tian, F., J. A. Losonczi, M. W. F. Fischer, and J. H. Prestegard. 1999. Sign determination of dipolar couplings in field-oriented bicelles by variable angle sample spinning (VASS). *J. Biomol. NMR*. 15:145–150.

Vaananen, T., J. Jokisaari, and M. Selantaus. 1987. A variable-angle spinning system for the determination of NMR parameters of liquid-crystalline samples. *J. Magn. Reson*. 72:414–421.

van Paridon, P. A., B. de Kruijff, R. Ouwerkerk, and K. W. A. Wirtz. 1986. Polyphosphoinositides undergo charge neutralization in the physiological pH range: a ^{31}P-NMR study. *Biochim. Biophys. Acta*. 877:216–219.

Vinogradova, O., P. Badola, L. Czerski, F. D. Sonnichsen, and C. R. Sanders. 1997. *Escherichia coli* diacylglycerol kinase: a case study in the application of solution NMR methods to an integral membrane protein. *Biophys. J*. 72:2688–2701.

Vivekanandan, S., H. S. V. Deepak, G. A. N. Gowda, K. V. Ramanathan, and C. L. Khetrapal. 2002. NMR spectra of mixed liquid crystals of opposite diamagnetic susceptibility anisotropies near critical point under variable angle sample spinning. *J. Mol. Struct.* 602–603:485–489.

Wang, J., J. Denny, C. Tian, S. Kim, Y. Mo, F. Kovacs, Z. Song, K. Nishimura, Z. Gan, R. Fu, J. R. Quine, and T. A. Cross. 2000. Imaging membrane protein helical wheels. *J. Magn. Reson.* 114:162–167.

Zandomeneghi, G., M. Tomaselli, P. T. F. Williamson, and B. H. Meier. 2003a. NMR of bicelles: orientation and mosaic spread of the liquid crystal director under sample rotation. *J. Biomol. NMR*. 25:113–123.

Zandomeneghi, G., P. T. F. Williamson, A. Hunkeler, and B. H. Meier. 2003b. Switched-angle spinning applied to bicelles containing phospholipid-associated peptides. *J. Biomol. NMR*. 25:125–132.